Heralded single-photon source based on superpositions of squeezed states

Hiroo Azuma,[1,*] William J. Munro,[2] and Kae Nemoto[2,1]
[1]*Global Research Center for Quantum Information Science, National Institute of Informatics, 2-1-2 Hitotsubashi, Chiyoda-ku, Tokyo 101-8430, Japan*
[2]*Okinawa Institute of Science and Technology Graduate University, Onna-son, Okinawa 904-0495, Japan*

(Received 26 February 2024; accepted 2 May 2024; published 15 May 2024)

We propose a heralded single-photon source based on injecting a superposition of oppositely squeezed states onto a beam splitter. Our superposition of squeezed states is composed of only even photon number states (the number of photons is equal to $2, 6, 10, \ldots$) meaning the probability for an emitted single photon given as a heralded single-photon event is higher than what one can achieve from the usual two-mode squeezed state. This enables one to realize an enhanced heralded single-photon source. We discuss how to create this superposition of squeezed states utilizing a single-mode squeezed state and the cross-Kerr nonlinearity. Our proposed method significantly improves the probability of emitting the heralded single photon compared to spontaneous parametric down-conversion.

DOI: 10.1103/PhysRevA.109.053711

I. INTRODUCTION

Single-photon sources are essential tools in many quantum information-based technologies including quantum key distribution protocols [1] and linear optical quantum computation [2,3]. As such there has been significant world-wide effort to propose and demonstrate on-demand single-photon emitters. Quantum dots [4–8], nitrogen-vacancy centers in diamond [9–11], and negative silicon vacancy centers in diamond [12–14] have been proposed as solid state devices for realizing such emitters. Further cavity QED systems have been considered as a triggered single-photon source [15–18], but the current work horse is still spontaneous parametric down-conversion (SPDC) where we trigger off the idler photon [19–24]. However, the photon pair emission rate is low [4×10^{-6} per pump photon using a periodically poled lithium niobate (PPLN) waveguide [25]].

Implementation of heralded single-photon sources with the SPDC is state-of-the-art technology and is being studied with great effort currently [26]. A review of the heralded single-photon sources was given in [27,28]. Improvement of the heralded single-photon source with photon-number-resolving detectors was examined in Refs. [29,30]. Suppression of multiphoton events in a cavity-enhanced SPDC via the photon-blockade effect for the heralded single-photon source has been proposed [31], and a technique of heralding based on the detection of zero photons was investigated [32].

The essence of the heralded single-photon source is the generation of pairs of photons and is the reason we use SPDC. A more efficient method for generating entangled photons is the injection of squeezed light into a 50-50 beam splitter [33]. The resulting two-mode squeezed state source can in principle generate pairs of photons with a much higher success probability. Using an imperfect single-photon detector whose efficiency is equal to 0.9, the pure two-mode squeezed state with a squeezing parameter 0.5 gives the photon pair emission rate 0.151. There is, however, still room for improvement.

In this paper we introduce a more efficient approach based on superpositions of squeezed states. We investigate how to generate a pair of photons by injecting an odd superposition of squeezed states onto a 50-50 beam splitter [34]. In particular we show that we can create this superposition using a single-mode squeezed state source and a cross-Kerr nonlinear medium, although its heralded success probability is less than $1/2$ [35,36]. Finally, we determine the second-order intensity correlation functions $g^{(2)}(0)$ for the single-photon emissions of the superposition of oppositely squeezed states and the two-mode squeezed state. We use the measure $g^{(2)}(0)$ to evaluate whether or not the physical properties of a given photon source are close to those of an on-demand single-photon source [37].

This article is organized as follows. In Sec. II we begin by discussing the generation of a pair of photons using our superposition of oppositely squeezed states determining in Secs. II A and II B the probability and conditional probability of emission of the heralded single-photon source. Then in Sec. II C we consider errors induced by imperfect operations of devices. Next in Sec. III we compare our proposed heralded source with that from the pure two-mode squeezed state. In Sec. IV we determine the second-order intensity correlation functions for our source using imperfect single-photon detectors. Finally in Sec. V we provide a brief concluding discussion.

II. PHOTON PAIR GENERATION FROM A SUPERPOSITION OF OPPOSITELY SQUEEZED STATES

Let us begin by discussing our scheme for producing the superposition of the oppositely squeezed states using a

*zuma@nii.ac.jp

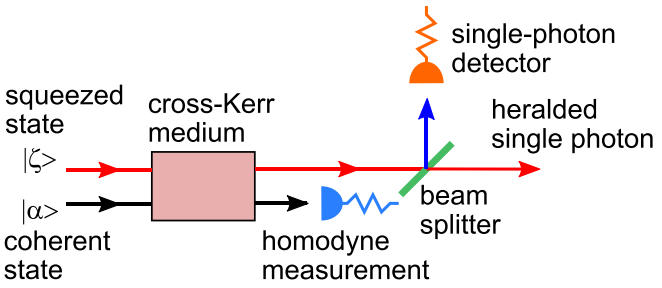

FIG. 1. Schematic illustration of a heralded single-photon source using a squeezed state and a cross-Kerr medium.

nonlinear cross-Kerr medium. This is depicted in Fig. 1. First, we prepare a two-mode initial state where the first and second modes are given by a squeezed state $|r\rangle = \hat{S}(r)|0\rangle$ and a coherent state $|\alpha\rangle$, respectively, as

$$|r\rangle_1 = \frac{1}{\sqrt{\cosh r}} \sum_{n=0}^{\infty} \frac{\sqrt{(2n)!}}{2^n n!} (-\tanh r)^n |2n\rangle_1, \tag{1}$$

$$|\alpha\rangle_2 = \exp(-|\alpha|^2/2) \sum_{n=0}^{\infty} \frac{\alpha^n}{\sqrt{n!}} |n\rangle_2, \tag{2}$$

where $\hat{S}(r)$ is the squeezing operator and $\{|n\rangle : n = 0, 1, 2, \ldots\}$ represent the photon number states. Both of these states then interact with a nonlinear cross-Kerr interaction of the form $\hat{H}_{12} = \hbar\kappa \hat{a}_1^\dagger \hat{a}_1 \hat{a}_2^\dagger \hat{a}_2$, where $\hat{a}_1$ and $\hat{a}_2$ are annihilation operators of modes 1 and 2, respectively. Formally the squeezing operator can be written as $\hat{S}(r) = \exp[(-r/2)(\hat{a}^{\dagger 2} - \hat{a}^2)]$. Our initial state $|\Psi_{\rm in}\rangle_{12} = |r\rangle_1 |\alpha\rangle_2$ evolves over a time τ to

$$|\Psi_{\rm out}\rangle_{12} = \frac{1}{\sqrt{\cosh r}} \sum_{n=0}^{\infty} \frac{\sqrt{(2n)!}}{2^n n!} (-\tanh r)^n |2n\rangle_1 |\alpha e^{-i2n\kappa\tau}\rangle_2. \tag{3}$$

Setting $2\kappa\tau = \pi$ we have

$$|\Psi_{\rm out}\rangle_{12} = \frac{1}{2}\mathcal{N}_+(r)^{1/2} |r;+\rangle_1 |\alpha\rangle_2 + \frac{1}{2}\mathcal{N}_-(r)^{1/2} |r;-\rangle_1 |-\alpha\rangle_2, \tag{4}$$

where

$$|r;\pm\rangle = \frac{|r\rangle \pm |-r\rangle}{\sqrt{\mathcal{N}_\pm(r)}}, \tag{5}$$

with

$$\mathcal{N}_\pm(r) = 2\left(1 \pm \frac{1}{\cosh r \sqrt{1 + \tanh^2 r}}\right). \tag{6}$$

The states $|r;+\rangle$ and $|r;-\rangle$ are superpositions of the photon number states $\{|2n\rangle : n = 0, 2, 4, \ldots\}$ and $\{|2n\rangle : n = 1, 3, 5, \ldots\}$, respectively.

Next, distinguishing $|\alpha\rangle_2$ and $|-\alpha\rangle_2$ by homodyne measurement, we project our system to either $|r;+\rangle$ or $|r;-\rangle$ with probability $\mathcal{N}_\pm(r)/4$, respectively. In general, $|\alpha\rangle$ and $|-\alpha\rangle$ are never perfectly orthogonal but $|\langle\alpha|-\alpha\rangle|^2 \leqslant 0.0012$ for $|\alpha| > 1.3$. Here we assume that $|\alpha|$ is sufficiently large. With the squeezing parameter $r = 0.725$ (corresponding to a squeezing level of 6.3 dB), $\mathcal{N}_+(r)/4$ and $\mathcal{N}_-(r)/4$ are equal to 0.833 and 0.167, respectively. It is worth mentioning that this probability $\mathcal{N}_-(r)/4$ monotonically increases from 0 to 1/2 as r goes to infinity.

In our scheme, we assume that we have a stable source of squeezed states $|r\rangle$, as the generation of squeezed states is a mature technology. A typical squeezing level of squeezed light used for experiments is given by 6.3 dB, which corresponds to the squeezing parameter $|r| = 0.725$ [38]. In the current paper, we typically use this parameter for showing examples but note that the detection of a 15 dB squeezed state of light was demonstrated experimentally [39].

In the proposed method, it is critical to adjust the duration of the nonlinear interaction time τ. To realize a precise adjustment of τ, we can fabricate a cavity of the cross-Kerr nonlinear medium, which is caught between two half-silvered mirrors. We can vary τ by changing the transmittance of mirrors. To obtain the phase factor $e^{-i2n\kappa\tau}$ with $2\kappa\tau = \pi$ for Eq. (3) precisely, κ must be large enough.

A. Heralded single-photon probability and conditional probability

Now let us establish the probability of successfully emitting our heralded single photon. We input the superposition of oppositely squeezed states $|r;\pm\rangle_a$ into one port of a 50-50 beam splitter with the vacuum on the second as depicted in Fig. 1. The incident squeezed field is transformed to

$$|r;\pm\rangle_a |0\rangle_b \to \mathcal{N}_\pm(r)^{-1/2} \Big[\hat{S}_{ab}\Big(-\frac{r}{2}\Big) \hat{S}_a\Big(\frac{r}{2}\Big) \hat{S}_b\Big(\frac{r}{2}\Big) \pm \hat{S}_{ab}\Big(\frac{r}{2}\Big) \hat{S}_a\Big(-\frac{r}{2}\Big) \hat{S}_b\Big(-\frac{r}{2}\Big) \Big] |0\rangle_a |0\rangle_b, \tag{7}$$

where $\hat{S}_{ab}(\pm r/2) = \exp[(\pm r/2)(\hat{a}^\dagger \hat{b}^\dagger - \hat{a}\hat{b})]$ are the origins of the entanglement between the modes.

Next the probability we can detect n_a photons at one output port and n_b at the other is given by

$$P(n_a, n_b; r; \pm) = \mathcal{N}_\pm(r)^{-1} |\langle n_a, n_b| \hat{S}_{ab}\Big(-\frac{r}{2}\Big) \hat{S}_a\Big(\frac{r}{2}\Big) \times \hat{S}_b\Big(\frac{r}{2}\Big) |0\rangle_a |0\rangle_b \pm \langle n_a, n_b| \hat{S}_{ab}\Big(\frac{r}{2}\Big) \times \hat{S}_a\Big(-\frac{r}{2}\Big) \hat{S}_b\Big(-\frac{r}{2}\Big) |0\rangle_a |0\rangle_b|^2. \tag{8}$$

In contrast, if we input an initial state $|r\rangle_a |0\rangle_b = \hat{S}_a(r)|0\rangle_a |0\rangle_b$ onto the beam splitter, the probability is

$$P(n_a, n_b; r) = |\langle n_a, n_b| \hat{S}_{ab}\Big(-\frac{r}{2}\Big) \hat{S}_a\Big(\frac{r}{2}\Big) \hat{S}_b\Big(\frac{r}{2}\Big) |0_a, 0_b\rangle|^2. \tag{9}$$

We can then define our conditional probabilities $P_{\rm c}(r;\pm)$ and $P_{\rm c}(r)$ as

$$P_{\rm c}(r;\pm) = P(1,1;r;\pm) \Big/ \sum_{n=0}^{\infty} P(1,n;r;\pm), \tag{10}$$

$$P_{\rm c}(r) = P(1,1;r) \Big/ \sum_{n=0}^{\infty} P(1,n;r). \tag{11}$$

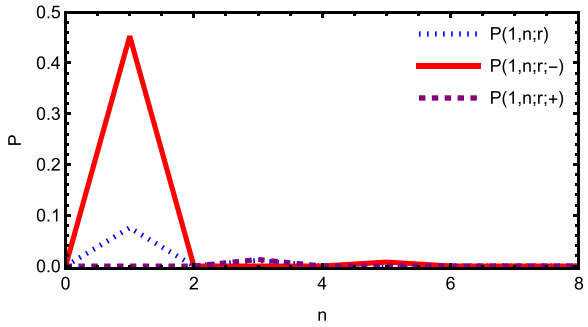

FIG. 2. Plot of the probability $P(1, n; r)$ and $P(1, n; r; \pm)$. We generate an n photon state $|n\rangle$ in one mode and a heralding photon in the other for the injected states $|r\rangle_a$ and $|r; \pm\rangle_a$ with $r = 0.725$. The dotted blue, solid red, and dashed purple line graphs represent $P(1, n; r)$, $P(1, n; r; -)$, and $P(1, n; r; +)$, respectively. The line graph of $P(1, n; r; +)$ overlaps the horizontal axis of n mostly.

If we observe $|\pm\alpha\rangle_2$ with the homodyne measurement, inject $|r; \pm\rangle_a$ into the beam splitter, and detect the heralding single photon in one port, we then obtain a single photon from the other port with probabilities $P_c(r; \pm)$. Thus, we can regard $P_c(r; \pm)$ as the conditional probabilities of single-photon emission after the postselection with the measurement outcomes on the other port. Similarly if we inject $|r\rangle_a$ into the beam splitter and detect the heralding single photon, we obtain a single photon with conditional probability $P_c(r)$.

B. Ideal single-photon detection

The photon after the beam splitter with $(n_a, n_b) = (1, 1)$ can be considered as a heralded single photon. When we generate $|r; \pm\rangle_1$ from $|r\rangle_1$, the probability that we obtain $|r; \pm\rangle_1$ is given by $\mathcal{N}_\pm(r)/4$. Thus, the actual probability for obtaining n_a and n_b photons from $|r; \pm\rangle_1$ is given by $\mathcal{N}_\pm(r)P(n_a, n_b; r; \pm)/4$.

In Fig. 2 we plot the probability $P(1, n; r)$ and $P(1, n; r; \pm)$ that we generate an n photon state $|n\rangle$ in one mode and a heralding photon in the other for the input states $|r\rangle_a$ and $|r; \pm\rangle_a$ with $r = 0.725$. Looking at Fig. 2, we note that $P(1, 1; r; -) = 0.453$, $P(1, 5; r; -) = 7.85 \times 10^{-3}$, and $P(1, n; r; -) = 0$ for $n = 0, 2, 3, 4$. Moreover, we obtain $P_c(r; -) = 0.983$. If we generate the superposition of the oppositely squeezed states $|r; -\rangle_a$, it should allow us to realize the heralded single-photon source with a high probability and so be a good alternative to the SPDC. By contrast, if we prepare the squeezed state $|r\rangle_a$, we obtain $P(1, 1; r) = 7.54 \times 10^{-2}$ with $P_c(r) = 0.859$. Looking at the plot of $|r; -\rangle$, the following question comes to mind. There must be an optimal value of r to maximize the probability. Answers to this question are shown in Fig. 3.

Next in Fig. 3(a), we plot the actual probability that we obtain the $|1\rangle$ photon Fock state conditioned that we observe a heralding single photon for the initial state $|r; -\rangle_a$. Examining Fig. 3(a), we note that $\mathcal{N}_-(r)P(1, 1; r; -)/4$ reaches its maximum value of 0.096 23 when $r = 1.146$. At that point the conditional probability is $P_c(1.146; -) = 0.9488$. Figure 3(b) shows plots of the probabilities of the heralded single photon as a function of r. We observe that $P_c(r; -)$

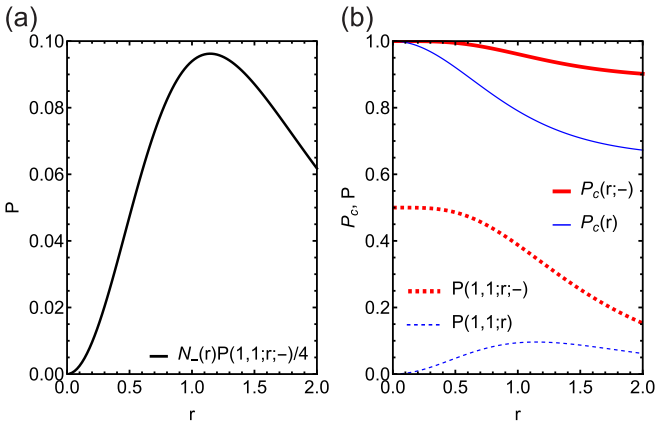

FIG. 3. (a) Plot of the probability $\mathcal{N}_-(r)P(1, 1; r; -)/4$. We obtain a heralded single photon by injecting $|r; -\rangle_a$ for $0 \leqslant r \leqslant 2$. When $r = 1.146$, the graph reaches its maximum value 0.096 23. Thus, the optimal value of r to maximize the probability is $r = 1.146$. (b) Plot of the probabilities of the heralded single photon as functions of r. The thick solid red and thin solid blue curves represent $P_c(r; -)$ and $P_c(r)$, respectively. The thick dashed red and thin dashed blue curves represent $P(1, 1; r; -)$ and $P(1, 1; r)$, respectively.

is larger than or equal to $P_c(r)$ for any r. Thus, as the heralded single-photon source, the superposition of oppositely squeezed states $|r; -\rangle$ is preferable to the typical squeezed state. It is useful to mention that the squeezed state $|r\rangle$ is a superposition of $\{|2n\rangle : n = 0, 1, 2, \ldots\}$ while contrastingly, the superpositions of the oppositely squeezed states $|r; +\rangle$ and $|r; -\rangle$ are superpositions of $\{|2m\rangle : m = 0, 2, 4, \ldots\}$ and $\{|2m\rangle : m = 1, 3, 5, \ldots\}$, respectively. The Fock states present in these superpositions of squeezed states are further separated in photon number space than the usual squeezed state. If we can prepare $|r; -\rangle \propto c_2|2\rangle + c_6|6\rangle + \ldots$ and inject that state into the 50-50 beam splitter, a transformation $|2\rangle_a|0\rangle_b \to (1/2)(|2\rangle_a|0\rangle_b + |0\rangle_a|2\rangle_b) - (1/\sqrt{2})|1\rangle_a|1\rangle_b$ occurs, and we obtain a state $|1\rangle_a|1\rangle_b$ with a maximal probability of 1/2. Hence, we can implement the heralded single-photon source with higher conditional probability. Figures 4(a) and 4(b) show 3D plots of the probabilities of generating $|r; -\rangle$ and

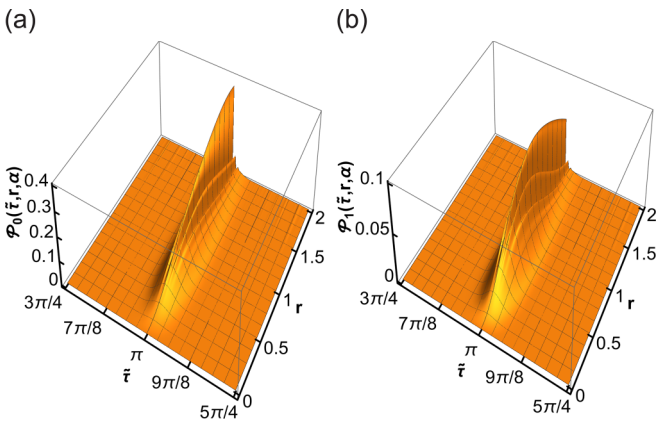

FIG. 4. (a) Plot of $\mathcal{P}_0(\tilde{\tau}, r, \alpha)$ as a function of $\tilde{\tau}$ and r with $\alpha = 10$. (b) Plot of $\mathcal{P}_1(\tilde{\tau}, r, \alpha)$ as a function of $\tilde{\tau}$ and r with $\alpha = 10$.

a heralded single photon as functions of $\tilde{\tau} = 2\kappa\tau$ and r, respectively, with fixing α at a specific value. In Fig. 4(a) we plot $\mathcal{P}_0$, the probability of generating $|r;-\rangle$, where

$$\mathcal{P}_0(\tilde{\tau}, r, \alpha) = |{}_{12}\langle\Psi_{\rm out}|r;-\rangle_1|-\alpha\rangle_2|^2. \tag{12}$$

In Fig. 4(b) we plot $\mathcal{P}_1$, the probability of generating a heralded single photon, where

$$\mathcal{P}_1(\tilde{\tau}, r, \alpha) = P(1,1,r;-)\mathcal{P}_0(\tilde{\tau}, r, \alpha). \tag{13}$$

Looking at both plots, we observe sharp peaks at $\tilde{\tau} = \pi$.

C. Imperfections and errors

In any realistic implementation, there will be imperfections, and so let us explore effects associated with the cross-phase modulation and also single-photon heralding detection. We have previously detailed the generation of $|r;-\rangle$ from the squeezed state $|r\rangle$ using the nonlinear cross-Kerr medium. For this generation, we had set duration τ for the nonlinear interaction as $2\kappa\tau = \pi$. Here we consider a case where an inaccuracy occurs; such timing is not perfect and a phase error could be induced as $2\kappa\tau = \pi + \Delta\theta$. In this case

$$|\Psi'_{\rm out}\rangle_{12} = \frac{1}{\sqrt{\cosh r}}\sum_{n=0}^{\infty}\frac{\sqrt{(2n)!}}{2^n n!}(-\tanh r)^n \times |2n\rangle_1|(-1)^n\alpha e^{-in\Delta\theta}\rangle_2, \tag{14}$$

where we assume α is real and greater than zero. To realize our heralded single-photon source, we want to generate a state of the form

$$|\Psi^{(-)}_{\rm out}\rangle_{12} = \frac{1}{2}\mathcal{N}_-(r)^{1/2}|r;-\rangle_1|-\alpha\rangle_2, \tag{15}$$

and so to evaluate the effects caused by $\Delta\theta$, we define the following ratio that implies the decrease in generation probability of $|r;-\rangle$ due to $\Delta\theta$:

$$R(r,\alpha,\Delta\theta) = \frac{|{}_{12}\langle\Psi^{(-)}_{\rm out}|\Psi'_{\rm out}\rangle_{12}|^2}{|{}_{12}\langle\Psi^{(-)}_{\rm out}|\Psi'_{\rm out}\rangle_{12}|^2\big|_{\Delta\theta=0}}. \tag{16}$$

Here $\Delta\theta$ is not a constant value but a probabilistic random variable that obeys Gaussian distribution whose mean value and standard deviation are given by zero and σ, respectively. Taking the average of $R(r,\alpha,\Delta\theta)$ with varying $\Delta\theta$ for many samples, we numerically obtain

$$R(r,\alpha,\sigma) = \int_{-\infty}^{\infty} d(\Delta\theta)\frac{1}{\sqrt{2\pi\sigma^2}}\exp\left(-\frac{\Delta\theta^2}{2\sigma^2}\right)R(r,\alpha,\Delta\theta). \tag{17}$$

In Fig. 5(a) we plot $R(r,\alpha,\sigma)$ for $\alpha = 9$, 10, and 11 with $r = 0.725$. In the range of $0 \leqslant \sigma \leqslant 0.001$, the function $\exp(-\lambda\sigma^2)$ approximates to the curves of $R(r,\alpha,\sigma)$ well. Looking at those plots, we note that the curve of $R(r,\alpha,\sigma)$ gets closer to a horizontal as α becomes smaller. Thus, we become aware that the error of the inaccuracy of the duration is serious for large α. Because the homodyne measurement requires a strong coherent state, we need to increase $|\alpha|$ for precise measurements. However, large $|\alpha|$ makes the single-photon emission vulnerable to the inaccuracy of duration τ, and a trade-off emerges. Figure 5(b) shows a 3D plot of $R(r,\alpha,\sigma)$ with $\alpha = 10$ as a function of r and σ where we

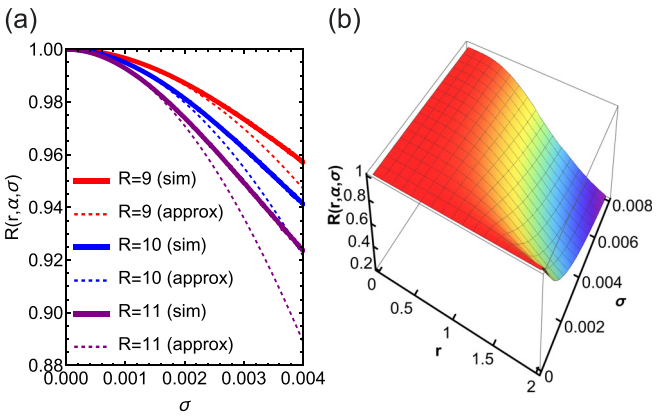

FIG. 5. (a) Plot of $R(r,\alpha,\sigma)$ as a function of σ for $r = 0.725$ and $\alpha = 9$ (thick solid red line), 10 (thick dashed blue line), and 11 (thick dotted purple lines), respectively. The thin solid red, thin dashed blue, and thin dotted purple curves represent functions $\exp(-\lambda\sigma^2)$ for $\lambda = 3401 \pm 3$, 5102 ± 2, and 7360 ± 4, respectively, that approximate the curves of $R(r,\alpha,\sigma)$ well for small r. (b) 3D plot of $R(r,\alpha,\sigma)$ as a function of both r and σ for $\alpha = 10$. In the regime where r is larger than $1/2$, $R(r,\alpha,\sigma)$ decreases as σ gets larger.

note that, in the range where r is larger than $1/2$, $R(r,10,\sigma)$ decreases as σ gets larger. Fluctuations of the phase error are problematic when we try to obtain strong squeezing. If we want to generate a strongly squeezed state, we must ensure the accuracy of the cross-Kerr phase modulation giving us another trade-off.

In Fig. 5(a) $R(r,\alpha,\sigma)$ departs from unity considerably for $\sigma = 0.004$. This standard deviation corresponds to a fluctuation $\Delta\tau = \tau\sigma/\pi$. This evaluation suggests to us that we must fix τ with the accuracy $\Delta\tau/\tau \sim 10^{-3}$, and it is well within our reach experimentally.

Next, we consider inefficient single-photon detection. So far we have assumed that we can use an ideal single-photon detector for the heralding measurement. The implementation of the single-photon detector is a cutting-edge technology with detection efficiencies above 90% regularly reported [40,41].

We can model a "click/no click" detector of efficiency η by the POVM $\{\hat{M}, \hat{\boldsymbol{I}} - \hat{M}\}$ [3,42,43], where

$$\hat{M} = \eta\sum_{k=1}^{\infty}(1-\eta)^{k-1}|k\rangle\langle k|, \tag{18}$$

for a "click" and $\hat{\boldsymbol{I}} - \hat{M}$ for "no click". If we use our quantum state $|r;-\rangle$ for a heralded single-photon source, the click probability is then

$$P_{\rm click}(r,\eta;-) = \eta\sum_{n_a=1}^{\infty}\sum_{m_b=0}^{\infty}(1-\eta)^{n_a-1}P(n_a,m_b;r;-). \tag{19}$$

The probability that the detector "clicks" and the heralded single photon is actually emitted is given by

$$P_{{\rm click},1}(r,\eta;-) = \eta\sum_{n_a=1}^{\infty}(1-\eta)^{n_a-1}P(n_a,1;r;-). \tag{20}$$

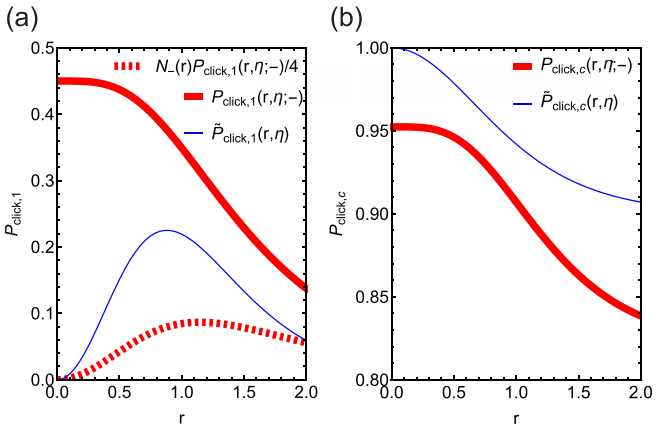

FIG. 6. (a) Plot of $P_{\text{click},1}(r,\eta;-)$, $\tilde{P}_{\text{click},1}(r,\eta)$ defined in Eq. (25), and $\mathcal{N}_-(r)P_{\text{click},1}(r,\eta;-)/4$ as a function of r for $\eta = 0.9$, where they are represented by the thick solid red, thin solid blue, and thick dashed red curves, respectively. (b) Plot of $P_{\text{click,c}}(r,\eta;-)$ and $\tilde{P}_{\text{click,c}}(r,\eta)$ defined in Eq. (26) as a function of r with $\eta = 0.9$, where they are represented by the thick red and thin blue curves, respectively.

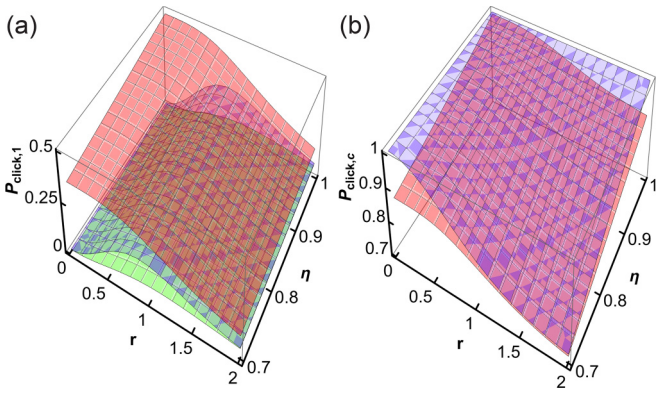

FIG. 7. (a) 3D plots of $P_{\text{click},1}(r,\eta;-)$, $\tilde{P}_{\text{click},1}(r,\eta)$, and $\mathcal{N}_-(r)P_{\text{click},1}(r,\eta;-)/4$ as functions of r and η, where they are represented by the curved red, blue, and green transparent surfaces, respectively. (b) 3D plots of $P_{\text{click,c}}(r,\eta;-)$ and $\tilde{P}_{\text{click,c}}(r,\eta)$ as functions of r and η, where they are represented by the curved red and blue transparent surfaces, respectively. In the regime $r \leqslant 2$ and $0.7 \leqslant \eta \leqslant 1$ we have $P_{\text{click},1}(r,\eta;-) > \tilde{P}_{\text{click},1}(r,\eta) > \mathcal{N}_-(r)P_{\text{click},1}(r,\eta;-)/4$ and $P_{\text{click,c}}(r,\eta;-) < \tilde{P}_{\text{click,c}}(r,\eta)$.

Then we can compute the conditional probability as

$$P_{\text{click,c}}(r,\eta;-) = \frac{P_{\text{click},1}(r,\eta;-)}{P_{\text{click}}(r,\eta;-)}. \tag{21}$$

In Fig. 6(a) we plot $P_{\text{click},1}(r,\eta;-)$ and $\mathcal{N}_-(r)P_{\text{click},1}(r,\eta;-)/4$ as functions of r for $\eta = 0.9$, where $\mathcal{N}_-(r)P_{\text{click},1}(r,\eta;-)/4$ is the probability that the heralded single photon is actually emitted. Although the single-photon detector is imperfect ($\eta = 0.9$), $P_{\text{click},1}(r,\eta;-)$ is nearly equal to 0.5 for the small squeezing parameter r. This is one of the advantages that our method has.

In Fig. 6(b) we plot $P_{\text{click,c}}(r,\eta;-)$ as a function of r for $\eta = 0.9$. This plot shows that $P_{\text{click,c}}(r,\eta;-)$ is nearly equal to 0.95 at $r = 0$ and decreases gradually as r becomes larger. In Fig. 7(a) we plot $P_{\text{click},1}(r,\eta;-)$ and $\mathcal{N}_-(r)P_{\text{click},1}(r,\eta;-)/4$ as functions of r and η, where $\mathcal{N}_-(r)P_{\text{click},1}(r,\eta;-)/4$ is the probability that the heralded single photon is actually emitted. In the limit of $r \to 0$, $P_{\text{click},1}(r,\eta;-)$ is finite and nonzero, but $\mathcal{N}_-(r)P_{\text{click},1}(r,\eta;-)/4$ approaches zero. In Fig. 7(b) we plot $P_{\text{click,c}}(r,\eta;-)$ as a function of r and η. As r increases and η decreases, $P_{\text{click,c}}(r,\eta;-)$ becomes smaller gradually.

III. COMPARISON WITH A HERALDED SINGLE-PHOTON SOURCE FROM THE TWO-MODE SQUEEZED STATE

Let us now review the generation of a heralded single photon using the pure two-mode squeezed state for comparison with our proposed method. Injecting two squeezed states individually onto a 50-50 beam splitter allows us to create the two-mode squeezed state

$$|r\rangle_a|r\rangle_b \to \hat{S}_{ab}(ir)|0\rangle_a|0\rangle_b, \tag{22}$$

where r is real. The probability we detect n_a photons and n_b photons is given by

$$\tilde{P}(n_a,n_b;r) = \left|\langle n_a,n_b|\hat{S}_{ab}(ir)|0_a,0_b\rangle\right|^2, \tag{23}$$

meaning that we can write the probability for $n_a = 1$ as $\tilde{P}(1,n_b;r) = (\tanh r/\cosh r)^2\delta_{n_b,1}$. If we observe a single photon in the first output mode, we obtain a single photon in the second output mode deterministically.

In Fig. 8 we plot $P(1,1;r;-)$, $\tilde{P}(1,1;r)$, and $\mathcal{N}_-(r)P(1,1;r;-)/4$ as a function of r. When $r = \text{arcsech}(1/\sqrt{2}) = 0.881$, $\tilde{P}(1,1;r)$ achieves its maximum value of 1/4. In the limit of $r \to 0$, $P(1,1;r;-)$ and $\tilde{P}(1,1;r)$ approach 1/2 and 0, respectively. In the limit of $r \to 0$, both $\mathcal{N}_-(r)P(1,1;r;-)/4$ and $\tilde{P}(1,1;r)$ approach zero, sharing

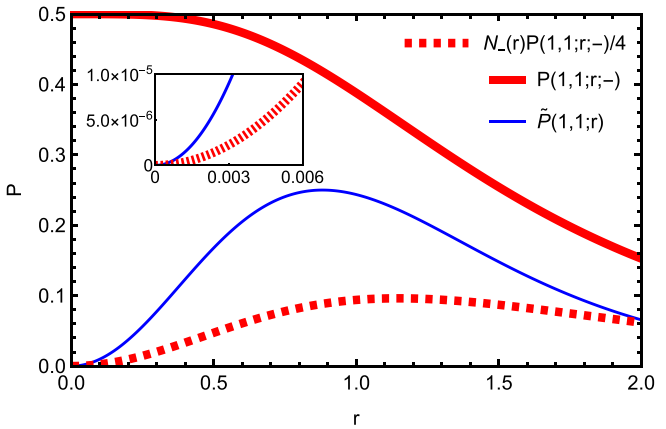

FIG. 8. Plot of $P(1,1;r;-)$, $\tilde{P}(1,1;r)$, and $\mathcal{N}_-(r)P(1,1;r;-)/4$ as functions of r which are represented as the thick solid red, thin solid blue, and thick dashed red curves, respectively. The graph of $\tilde{P}(1,1;r)$ reaches the maximum value 1/4 for $r = \text{arcsech}(1/\sqrt{2}) = 0.881$ and reaches the minimum value 0 for $r = 0$. We put a small frame of plots of $\mathcal{N}_-(r)P(1,1;r;-)/4$ and $\tilde{P}(1,1;r)$ for $0 \leqslant r \leqslant 0.006$ in the main frame. These plots show that $\mathcal{N}_-(r)P(1,1;r;-)/4$ and $\tilde{P}(1,1;r)$ are larger than 4×10^{-6} for $r \geqslant 0.004$. Thus, the heralded single-photon sources of our scheme and the pure two-mode squeezed state are more efficient than the SPDC even for small squeezing parameter r.

the same defect. However, in a practical circumstance where the squeezing parameter r is small, our scheme with the postselection of measuring $|-\alpha\rangle_2$ shown in Fig. 1 gives the probability $P(1,1;r;-)$ to be nearly equal to $1/2$ around $r=0$. Hence, the superposition of oppositely squeezed states $|r;-\rangle$ is preferable to the pure two-mode squeezed state $\hat{S}_{ab}(ir)|0\rangle_a|0\rangle_b$ as a source of the heralded single photons.

Now if we prepare a factory where we can produce many light beams of $|r;-\rangle$ by the cross-Kerr nonlinear medium and the homodyne measurements, we obtain heralded single photons efficiently for small r because of $\lim_{r\to 0} P(1,1;r;-)=0.5$. Moreover, looking at Fig. 3(b), we note that the conditional probability $P_c(r;-)$ is close to unity for small r. Hence, if we construct the heralded single-photon source with $|r;-\rangle$, the emission of the single photons is nearly deterministic. Contrastingly, if we use the pure two-mode squeezed state $\hat{S}_{ab}(ir)|0\rangle_a|0\rangle_b$ for the heralded single-photon source, we cannot obtain the emission of the single photons efficiently because $\lim_{r\to 0}\tilde{P}(1,1;r)=0$. In Fig. 8 we note that $\tilde{P}(1,1;r)<P(1,1;r;-)$ for $0\leqslant r\leqslant 2$. Thus, $|r;-\rangle_a$ is preferable to $\hat{S}_{ab}(ir)|0\rangle_a|0\rangle_b$. Although we always obtain the heralded single photon when we detect the heralding single photon for the two-mode squeezed state and its conditional probability is exactly equal to unity, looking at Fig. 3(b), we observe that $P_c(r;-)$ is nearly and sufficiently equal to unity, as well. Thus, regarding the conditional probabilities, the superposition of oppositely squeezed states $|r;-\rangle$ is as useful as the pure two-mode squeezed state.

Next, we consider the case where the single-photon detector is imperfect, and its "click" operator is given by Eq. (18). In this case, the click probability is

$$\tilde{P}_{\rm click}(r,\eta)=\frac{2\eta\tanh^2 r}{2-\eta[1-\cosh(2r)]}. \tag{24}$$

The probability that the detector observes the click operator $\hat{M}$ and the heralded single photon is actually emitted is given by

$$\tilde{P}_{{\rm click},1}(r,\eta)=\eta\frac{\tanh^2 r}{\cosh^2 r}. \tag{25}$$

Then, we can compute the conditional probability as

$$\tilde{P}_{\rm click,c}(r,\eta)=\frac{\tilde{P}_{{\rm click},1}(r,\eta)}{\tilde{P}_{\rm click}(r,\eta)}=\eta+(1-\eta)\cosh^{-2} r. \tag{26}$$

In Figs. 6(a) and 6(b), we plot $\tilde{P}_{{\rm click},1}(r,\eta)$ and $\tilde{P}_{\rm click,c}(r,\eta)$ as functions of r for $\eta=0.9$ while in Figs. 7(a) and 7(b), we plot $\tilde{P}_{{\rm click},1}(r,\eta)$ and $\tilde{P}_{\rm click,c}(r,\eta)$ as functions of r and η. Figure 6(a) shows that $\tilde{P}_{{\rm click},1}(r,\eta)$ is nearly equal to zero for small r. This characteristic is in contrast to our proposed method because $P_{{\rm click},1}(r,\eta;-)$ is larger than 0.4 for small r. Comparing $P_{\rm click,c}(r,\eta;-)$ and $\tilde{P}_{\rm click,c}(r,\eta)$ in Fig. 6(b), we cannot find a large difference between them for small r. For this point, both methods are comparable. Examining Fig. 7(a), we note that $P_{{\rm click},1}(r,\eta;-)$ is larger than $\tilde{P}_{{\rm click},1}(r,\eta)$ for $0\leqslant r\leqslant 2$ and $0.7\leqslant\eta\leqslant 1$. Moreover, $\lim_{r\to 0}P_{{\rm click},1}(r,\eta;-)>0$ and $\lim_{r\to 0}\tilde{P}_{{\rm click},1}(r,\eta)=0$ hold. Thus, for most realistic cases, the superposition of oppositely squeezed states is more beneficial to the heralded single-photon emission than the pure two-mode squeezed state. Looking at Fig. 7(b), we note that $P_{\rm click,c}(r,\eta;-)<\tilde{P}_{\rm click,c}(r,\eta)$ for $0\leqslant r\leqslant 2$ and $0.7\leqslant\eta\leqslant 1$. However, for larger r and smaller η the difference is small.

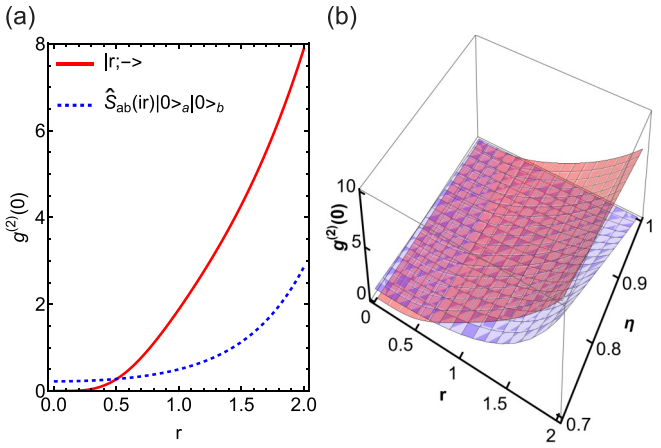

FIG. 9. (a) Plot of $g^{(2)}(0)$ for $|r;-\rangle$ (solid red curve) and $\hat{S}_{ab}(ir)|0\rangle_a|0\rangle_b$ (dashed blue curve) as a function of r with $\eta=0.9$. (b) Plot of $g^{(2)}(0)$ as a function of r and η.

IV. THE SECOND-ORDER INTENSITY CORRELATION FUNCTIONS

Now we consider the second-order intensity correlation functions $g^{(2)}(0)$ for the heralded single-photon emitters realized with the superposition of oppositely squeezed states $|r;-\rangle$ and the pure two-mode squeezed state $\hat{S}_{ab}(ir)|0\rangle_a|0\rangle_b$. We can measure the quality of the single-photon source by

$$g^{(2)}(0)=\frac{\langle n(n-1)\rangle}{\langle n\rangle^2}. \tag{27}$$

When an on-demand identical photon gun is realized, we obtain $g^{(2)}(0)=0$. For our proposed method, we have to calculate $g^{(2)}(0)$ numerically. By contrast, for the pure two-mode squeezed state,

$$g^{(2)}(0)=-3+\frac{2}{\eta}+\eta+(1-\eta)\cosh 2r. \tag{28}$$

We plot $g^{(2)}(0)$ for $|r;-\rangle$ and $\hat{S}_{ab}(ir)|0\rangle_a|0\rangle_b$ in Fig. 9. We observe that $g^{(2)}(0)$ is always less for $|r;-\rangle$ in the shown region. In particular for $|r;-\rangle$, we notice that $g^{(2)}(0)$ approaches zero as $r\to 0$, while for the two-mode squeezed state it is always greater than zero for $r\geqslant 0$. Thus, for $\eta=0.9$ and $0\leqslant r\leqslant 0.504$, the single-photon emitter realized by $|r;-\rangle$ has a better quality than the two-mode squeezed state. We can understand the reason why this difference emerges as follows. The state $|r;-\rangle$ is a superposition of photon-number states, $|2\rangle$, $|6\rangle$, $|10\rangle$,.... Thus, dividing the state $|r;-\rangle$ on two ports of a 50-50 beam splitter, the probability that the imperfect photon detector detects the state $|2\rangle_a$ is suppressed. Thus, $g^{(2)}(0)$ hardly suffers from an imperfection caused by the term $\eta(1-\eta)|2\rangle_{aa}\langle 2|$ included in the observable $\hat{M}$ given by Eq. (18). By contrast, the pure two-mode squeezed state is a superposition of the states, $|0\rangle_a|0\rangle_b$, $|1\rangle_a|1\rangle_b$, $|2\rangle_a|2\rangle_b$, ..., so

that it is vulnerable to the imperfect term $\eta(1-\eta)|2\rangle_{aa}\langle 2|$. In Fig. 9(b) we plot $g^{(2)}(0)$ as a function of r and η for $0 \leqslant r \leqslant 2$ and $0.7 \leqslant \eta \leqslant 1$. We observe that $g^{(2)}(0)$ for our odd superposition of squeezed states is always smaller than that associated with the two-mode squeezed state for small r. This fact implies that the heralded single-photon emitter realized by $|r;-\rangle$ is more robust than that realized by $\hat{S}_{ab}(ir)|0\rangle_a|0\rangle_b$ under the condition that we must use the imperfect single-photon detector. In Fig. 9(a) we note that $g^{(2)}(0)$ of the pure two-mode squeezed state exhibits partial stability around $g^{(2)}(0) = 0.22$ for $0 \leqslant r \leqslant 1.0$. In contrast, our proposed method can achieve a high quality of single photons for the small r regime ($0 \leqslant r \leqslant 0.504$). This regime of the squeezing parameter r is most relevant in the current experiment.

To compare our scheme with other single-photon sources, the method of the pure two-mode squeezed state in particular, we also need to count the probability of single-photon generation as shown in Fig. 3. When r is smaller than 0.504, the success probability of obtaining a single photon after the postselection is nearly equal to $1/2$, as shown by $P(1,1;r;-)$ in Fig. 3(b), hence both the success probability and the quality are high enough. However, as Fig. 3(a) indicates, the yielding of the success case is rather low when r approaches zero. The usual trade-off between purity and overall efficiency remains in our scheme [44,45].

V. CONCLUSION

In this paper we proposed a method to generate a heralded single-photon source created from a superposition of oppositely squeezed states. We outlined the method for producing this state by injecting squeezed and coherent light beams onto a cross-Kerr nonlinear medium and estimated the probability and conditional probability of the emission of the heralded single photons. To evaluate the quality of our proposed method, we used the pure two-mode squeezed state for comparison. When the single-photon detector detects the heralding signals inaccurately, our method shows better performance for the second-order intensity correlation function $g^{(2)}(0)$ than the method of the pure two-mode squeezed states for small r as explained in Sec. IV. This is because $|r\rangle - |-r\rangle$ is a superposition of photon-number states, $|2\rangle, |6\rangle, |10\rangle$, ...and the probability amplitude of $|n\rangle_a|2\rangle_b$ for $n = 0, 1, 2, \ldots$ is suppressed when we inject it into the 50-50 beam splitter. That is an important advantage of our scheme. However the generation of the odd superposition of squeezed states is more difficult leading to a natural trade-off.

ACKNOWLEDGMENTS

This work was supported by MEXT Quantum Leap Flagship Program Grant No. JPMXS0120351339.

[1] C. H. Bennett and G. Brassard, Quantum cryptography: Public key distribution and coin tossing, in *Proceedings of IEEE International Conference on Computers, Systems and Signal Processing, Bangalore, India* (IEEE, New York), pp. 175–179 (1984); Theor. Comput. Sci. **560**, 7 (2014).

[2] E. Knill, R. Laflamme, and G. J. Milburn, A scheme for efficient quantum computation with linear optics, Nature (London) **409**, 46 (2001).

[3] P. Kok, W. J. Munro, K. Nemoto, T. C. Ralph, J. P. Dowling, and G. J. Milburn, Linear optical quantum computing with photonic qubits, Rev. Mod. Phys. **79**, 135 (2007).

[4] O. Benson, C. Santori, M. Pelton, and Y. Yamamoto, Regulated and entangled photons from a single quantum dot, Phys. Rev. Lett. **84**, 2513 (2000).

[5] P. Michler, A. Kiraz, C. Becher, W. V. Schoenfeld, P. M. Petroff, L. Zhang, E. Hu, and A. Imamoğlu, A quantum dot single-photon turnstile device, Science **290**, 2282 (2000).

[6] C. Santori, M. Pelton, G. Solomon, Y. Dale, and Y. Yamamoto, Triggered single photons from a quantum dot, Phys. Rev. Lett. **86**, 1502 (2001).

[7] M. Pelton, C. Santori, J. Vučković, B. Zhang, G. S. Solomon, J. Plant, and Y. Yamamoto, Efficient source of single photons: A single quantum dot in a micropost microcavity, Phys. Rev. Lett. **89**, 233602 (2002).

[8] A. Kiraz, M. Atatüre, and A. Imamoğlu, Quantum-dot single-photon sources: Prospects for applications in linear optics quantum-information processing, Phys. Rev. A **69**, 032305 (2004); **70**, 059904(E) (2004).

[9] H. Bernien, L. Childress, L. Robledo, M. Markham, D. Twitchen, and R. Hanson, Two-photon quantum interference from separate nitrogen vacancy centers in diamond, Phys. Rev. Lett. **108**, 043604 (2012).

[10] R. Albrecht, A. Bommer, C. Deutsch, J. Reichel, and C. Becher, Coupling of a single nitrogen-vacancy center in diamond to a fiber-based microcavity, Phys. Rev. Lett. **110**, 243602 (2013).

[11] L. Liebermeister, F. Petersen, A. v. Münchow, D. Burchardt, J. Hermelbracht, T. Tashima, A. W. Schell, O. Benson, T. Meinhardt, A. Krueger *et al.*, Tapered fiber coupling of single photons emitted by a deterministically positioned single nitrogen vacancy center, Appl. Phys. Lett. **104**, 031101 (2014).

[12] L. J. Rogers, K. D. Jahnke, T. Teraji, L. Marseglia, C. Müller, B. Naydenov, H. Schauffert, C. Kranz, J. Isoya, L. P. McGuinness, and F. Jelezko, Multiple intrinsically identical single-photon emitters in the solid state, Nat. Commun. **5**, 4739 (2014).

[13] L. J. Rogers, K. D. Jahnke, M. W. Doherty, A. Dietrich, L. P. McGuinness, C. Müller, T. Teraji, H. Sumiya, J. Isoya, N. B. Manson, and F. Jelezko, Electronic structure of the negatively charged silicon-vacancy center in diamond, Phys. Rev. B **89**, 235101 (2014).

[14] J. Benedikter, H. Kaupp, T. Hümmer, Y. Liang, A. Bommer, C. Becher, A. Krueger, J. M. Smith, T. W. Hänsch, and D. Hunger, Cavity-enhanced single-photon source based on the silicon-vacancy center in diamond, Phys. Rev. Appl. **7**, 024031 (2017).

[15] A. Kuhn, M. Hennrich, T. Bondo, and G. Rempe, Controlled generation of single photons from a strongly coupled atom-cavity system, Appl. Phys. B **69**, 373 (1999).

[16] S. Brattke, B. T. H. Varcoe, and H. Walther, Generation of photon number states on demand via cavity quantum electrodynamics, Phys. Rev. Lett. **86**, 3534 (2001).

[17] M. Mücke, J. Bochmann, C. Hahn, A. Neuzner, C. Nölleke, A. Reiserer, G. Rempe, and S. Ritter, Generation of single photons from an atom-cavity system, Phys. Rev. A **87**, 063805 (2013).

[18] H. Azuma, Numerical analyses of emission of a single-photon pulse based on single-atom-cavity quantum electrodynamics, Prog. Theor. Exp. Phys. **2019**, 063A01 (2019).

[19] S. Fasel, O. Alibart, S. Tanzilli, P. Baldi, A. Beveratos, N. Gisin, and H. Zbinden, High-quality asynchronous heralded single-photon source at telecom wavelength, New J. Phys. **6**, 163 (2004).

[20] P. J. Mosley, J. S. Lundeen, B. J. Smith, P. Wasylczyk, A. B. U'Ren, Ch. Silberhorn, and I. A. Walmsley, Heralded generation of ultrafast single photons in pure quantum states, Phys. Rev. Lett. **100**, 133601 (2008).

[21] G. Brida, I. P. Degiovanni, M. Genovese, F. Piacentini, P. Traina, A. D. Frera, A. Tosi, A. B. Shehata, C. Scarcella, A. Gulinatti *et al.*, An extremely low-noise heralded single-photon source: A breakthrough for quantum technologies, Appl. Phys. Lett. **101**, 221112 (2012).

[22] S. Krapick, H. Herrmann, V. Quiring, B. Brecht, H. Suche, and Ch. Silberhorn, An efficient integrated two-color source for heralded single photons, New J. Phys. **15**, 033010 (2013).

[23] L. A. Ngah, O. Alibart, L. Labonté, V. D'Auria, and S. Tanzilli, Ultra-fast heralded single photon source based on telecom technology, Laser Photonics Rev. **9**, L1 (2015).

[24] F. Kaneda, B. G. Christensen, J. J. Wong, H. S. Park, K. T. McCusker, and P. G. Kwiat, Time-multiplexed heralded single-photon source, Optica **2**, 1010 (2015).

[25] M. Bock, A. Lenhard, C. Chunnilall, and C. Becher, Highly efficient heralded single-photon source for telecom wavelengths based on a PPLN waveguide, Opt. Express **24**, 23992 (2016).

[26] C. Kießler, H. Conradi, M. Kleinert, V. Quiring, H. Herrmann, and Ch. Silberhorn, Fiber-coupled plug-and-play heralded single photon source based on Ti:$LiNbO_3$ and polymer technology, Opt. Express **31**, 22685 (2023).

[27] S. A. Castelletto and R. E. Scholten, Heralded single photon sources: A route towards quantum communication technology and photon standards, Eur. Phys. J. Appl. Phys. **41**, 181 (2008).

[28] E. Meyer-Scott, Ch. Silberhorn, and A. Migdall, Single-photon sources: Approaching the ideal through multiplexing featured, Rev. Sci. Instrum. **91**, 041101 (2020).

[29] S. I. Davis, A. Mueller, R. Valivarthi, N. Lauk, L. Narvaez, B. Korzh, A. D. Beyer, O. Cerri, M. Colangelo, K. K. Berggren *et al.*, Improved heralded single-photon source with a photon-number-resolving superconducting nanowire detector, Phys. Rev. Appl. **18**, 064007 (2022).

[30] L. Stasi, P. Caspar, T. Brydges, H. Zbinden, F. Bussières, and R. Thew, High-efficiency photon-number-resolving detector for improving heralded single-photon sources, Quantum Sci. Technol. **8**, 045006 (2023).

[31] J. Tang, L. Tang, H. Wu, Y. Wu, H. Sun, H. Zhang, T. Li, Y. Lu, M. Xiao, and K. Xia, Towards on-demand heralded single-photon sources via photon blockade, Phys. Rev. Appl. **15**, 064020 (2021).

[32] C. M. Nunn, J. D. Franson, and T. B. Pittman, Heralding on the detection of zero photons, Phys. Rev. A **104**, 033717 (2021).

[33] M. S. Kim, W. Son, V. Bužek, and P. L. Knight, Entanglement by a beam splitter: Nonclassicality as a prerequisite for entanglement, Phys. Rev. A **65**, 032323 (2002).

[34] P. Marek, M. Paternostro, and M. S. Kim, Characterization of the entanglement of two squeezed states, Phys. Rev. A **74**, 032311 (2006).

[35] Y.-B. Sheng, F.-G. Deng, and H.-Y. Zhou, Efficient polarization-entanglement purification based on parametric down-conversion sources with cross-Kerr nonlinearity, Phys. Rev. A **77**, 042308 (2008); Erratum: Efficient polarization-entanglement purification based on parametric down-conversion sources with cross-Kerr nonlinearity [Phys. Rev. A 77, 042308 (2008)] **77**, 059902(E) (2008).

[36] S. Ding, G. Maslennikov, R. Hablützel, and D. Matsukevich, Cross-kerr nonlinearity for phonon counting, Phys. Rev. Lett. **119**, 193602 (2017).

[37] D. F. Walls and G. J. Milburn, *Quantum Optics* (Springer-Verlag, Berlin, 1994).

[38] T. Kashiwazaki, T. Yamashima, N. Takanashi, A. Inoue, T. Umeki, and A. Furusawa, Fabrication of low-loss quasi-single-mode PPLN waveguide and its application to a modularized broadband high-level squeezer, Appl. Phys. Lett. **119**, 251104 (2021).

[39] H. Vahlbruch, M. Mehmet, K. Danzmann, and R. Schnabel, Detection of 15 dB squeezed states of light and their application for the absolute calibration of photoelectric quantum efficiency, Phys. Rev. Lett. **117**, 110801 (2016).

[40] Z. L. Yuan, B. E. Kardynal, A. W. Sharpe, and A. J. Shields, High speed single photon detection in the near infrared, Appl. Phys. Lett. **91**, 041114 (2007).

[41] X. Jiang, M. A. Itzler, R. Ben-Michael, and K. Slomkowski, InGaAsP-InP avalanche photodiodes for single photon detection, IEEE J. Sel. Top. Quantum Electron. **13**, 895 (2007).

[42] K. J. Resch, J. S. Lundeen, and A. M. Steinberg, Experimental observation of nonclassical effects on single-photon detection rates, Phys. Rev. A **63**, 020102(R) (2001).

[43] M. K. Akhlaghi, A. H. Majedi, and J. S. Lundeen, Nonlinearity in single photon detection: Modeling and quantum tomography, Opt. Express **19**, 21305 (2011).

[44] A. Christ and Ch. Silberhorn, Limits on the deterministic creation of pure single-photon states using parametric down-conversion, Phys. Rev. A **85**, 023829 (2012).

[45] P. Senellart, G. Solomon, and A. White, High-performance semiconductor quantum-dot single-photon sources, Nat. Nanotechnol. **12**, 1026 (2017).